Continuum Model for Polymorphism of Bacterial Flagella

Srikanth V. Srigiriraju and Thomas R. Powers
Division of Engineering, Box D, Brown University, Providence, Rhode Island 02912, USA
(Received 25 February 2005; published 21 June 2005)

Bacterial flagellar filaments can abruptly change shape in response to mechanical load or changes in solution pH or ionic strength. These polymorphic transformations are an instance of a ubiquitous phenomenon, the spread of conformational change in large macromolecular assemblies. We propose a new theory for polymorphism, whose essential elements are two molecular switches and an elastic mismatch strain between the inner and outer cores of the filament. We calculate the phase diagram for helical and straight states, and the response of a helical filament to an external moment.

DOI: 10.1103/PhysRevLett.94.248101 PACS numbers: 87.15.−v, 46.70.Hg, 87.16.Qp

The helical flagellar filaments of *Esherichia coli* and *Salmonella typhimurium* provide striking examples of the spread of conformational change through a macromolecular structure. These filaments consist of tens of thousands of identical copies of a protein subunit called flagellin. It is thought that the helical shape arises because the subunits prefer to be in one of two inequivalent conformations [1,2]. Under normal physiological conditions and in the absence of mechanical loading, wild-type filaments are left-handed helices with a pitch of about 2.5 μm and helical diameter of about 0.5 μm [3]. This state is known as the normal state. Hydrodynamic torque can trigger polymorphic transformations, in which a right-handed helical state invades the normal left-handed state via the propagation of a front [4,5]. Two right-handed states, called semicoiled and curly, are typically seen in swimming bacteria [3]. The transition from normal to semicoiled changes the swimming direction of the bacterium [3]. Discontinuous transitions between helical states can also occur due to changes in solvent condition, such as pH [6]. Straight states [1] and coiled states that are curved but not twisted [6] are also observed.

In this Letter, we present a new theory for polymorphism in bacterial flagella. Since it is impractical to calculate the behavior of a filament using an all-atom approach, we construct a coarse-grained continuum rod model that reflects the essential mechanical properties of the subunits. Our theory addresses two questions, articulated by Asakura [1]: (i) how can identical protein subunits form a helix, and (ii) what is the mechanism for polymorphic transformation? In our theory, the helical shape arises from a mismatch of the preferred lattice spacing of the protein subunits in the inner and outer core. This picture leads to an energy landscape with several minima corresponding to straight or helical filaments. Changes in the material parameters or external load can change the relative energies of the different minima, leading to transitions from one state to another.

The flagellin subunits form a two-dimensional crystal on the surface of the filament, which is about 20 nm in diameter. These subunits can be grouped into 11 protofilaments which gradually wrap around each other. To achieve the variation in protofilament length required by the natural helical shape of a filament, Asakura supposed that each subunit has two stable conformations of slightly different size [1]. If all subunits are in the same conformation, then the filament is straight. Two straight states, L type and R type, have been observed [7]; the period of the subunits along the protofilaments is 0.8 Å shorter in R type than in L type. Since the protofilaments wind around the filament, a helical filament results when some of the protofilaments are in the short state, and some are in the long state. Calladine developed this idea further by modeling the subunits as linear springs with two rest lengths, and showing that the curvature of a filament varies sinusoidally with the number of protofilaments in the short state [2].

Electron microscopy has shown that the filament cross section consists of outer domains surrounding a core with outer and inner regions [8]. Both the outer core and the inner core are crucial for polymorphism. Mutations in the outer core can change the helical pitch and radius of the ground state [9]. Without the inner core, there is no polymorphic behavior, and the filaments are straight [10]. X-ray crystallography [11] and high-resolution electron cryomicroscopy [12] studies have led to the suggestion

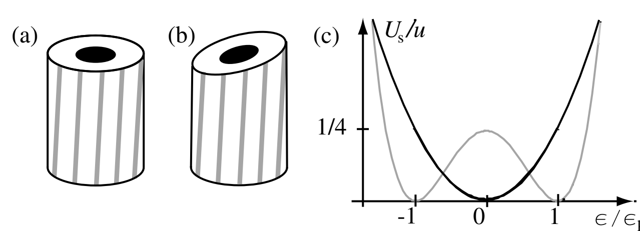

FIG. 1. (a) Filament element with $\epsilon_i = \epsilon = \epsilon_0$. The gray lines represent the strands and the black disk represents a cross section of the central spring. (b) Filament element with $\epsilon = \epsilon_0$, and a variation in the stretch ϵ_i of the strands. (c) Gray curve: energy vs stretch for a protofilament; black curve: energy vs stretch for the central spring (dimensionless units). For the situation in (c), (b) has lower energy than (a).

that there are two molecular switches underlying flagellar polymorphism: a highly cooperative switch for curvature, arising from the two slightly different subunit conformations, and a switch for twist, arising from lateral interactions between neighboring protofilaments [12].

Our aim is to create a continuum rod model for the flagellar filament, guided by these observations. The elements of our model are shown in Fig. 1(a). We approximate the filament structure by 11 strands wrapped around an elastic inner core. A strand is a nonlinear spring in the outer core, in contrast with the full protofilament which includes material in both the inner and outer cores. Each strand has a double-well potential (per unit length) for stretching,

$$U_{si} = \frac{u}{4}(\epsilon_i^2 - \epsilon_p^2)^2, \tag{1}$$

where ϵ_i is the strain of the ith strand [Fig. 1(c)]. The potential U_{si} has stable minima at $\epsilon_i = \pm\epsilon_p$, corresponding to the two conformations of a subunit. Since the difference in subunit spacing for L type and R type is ≈ 0.1 nm, and the subunit spacing is ≈ 5 nm, we estimate $2\epsilon_p \approx 1/50$. Because the two conformations are not symmetry-related, we do not expect the energy to have $\epsilon \mapsto -\epsilon$ symmetry. We consider the simplest case of a symmetric potential for purposes of illustration.

The inner core acts like a linear spring, with an elastic stretching energy per unit length

$$U_0 = \frac{1}{2}k_s(\epsilon - \epsilon_0)^2, \tag{2}$$

where ϵ is the strain of the inner core and ϵ_0 is the preferred strain. When $\epsilon_0^2 \neq \epsilon_p^2$, the central spring and the nonlinear springs have different preferred extensions, leading to an elastic mismatch strain.

To determine the strain of the strands given a configuration of the filament, we assume that planar cross sections remain planar when the filament is bent, twisted, or stretched (cf. [2]). These conditions are conveniently enforced using a material orthonormal frame $\{\hat{\mathbf{e}}_\mu\}$, where $\hat{\mathbf{e}}_3$ is the tangent vector of the filament, $\hat{\mathbf{e}}_1$ lies in the plane of the cross section and points from the center of the filament to the first protofilament, and $\hat{\mathbf{e}}_2 = \hat{\mathbf{e}}_3 \times \hat{\mathbf{e}}_1$. When the filament is bent or twisted, the frame $\{\hat{\mathbf{e}}_\mu\}$ rotates as the arclength s increases: $d\hat{\mathbf{e}}_\mu/ds = \boldsymbol{\kappa} \times \hat{\mathbf{e}}_\mu$, where $\boldsymbol{\kappa} = \kappa_\mu \hat{\mathbf{e}}_\mu$, κ_1 and κ_2 are the components of the curvature vector $\boldsymbol{\kappa}_\perp = \kappa_2\hat{\mathbf{e}}_1 - \kappa_1\hat{\mathbf{e}}_2$, and κ_3 is the twist. We relate the position of a material point $\mathbf{r}_i$ at radius a on the ith protofilament to the position of a point $\mathbf{r}_c$ on the centerline of the rod by $\mathbf{r}_i = \mathbf{r}_c + a\cos\beta_i\hat{\mathbf{e}}_1 + a\sin\beta_i\hat{\mathbf{e}}_2$, where $\beta_i \equiv 2\pi(i-1)/11$. Here a is chosen to be the radius at which the lattice structures of the straight filaments are reported [13], not the actual radius of the filament. Since $a = 4.5$ nm and the magnitudes of the κ_μ are all of order 1–10 $\mu\mathrm{m}^{-1}$, the strain is small, $\kappa_\mu a \ll 1$.

Now consider a filament which is bent, twisted, and stretched. To compute the strain in each strand, let S label material points of the inner core, and dl_i denote the length element of the ith strand: $dl_i = (d\mathbf{r}_i/dS \cdot d\mathbf{r}_i/dS)^{1/2}dS$. (The distinction between s and S must be recognized when computing the stretching strain. However, since $\epsilon \ll 1$, we may approximate $ds = (1+\epsilon)dS \approx dS$ in the measure for the energy integral and in the derivatives of the cooperative term described below.) To first order in $(\epsilon, a\kappa_\mu)$, the strain $\epsilon_i \equiv (dl_i - dS)/dS = \epsilon + a\kappa_1\sin\beta_i - a\kappa_2\cos\beta_i$. The twist does not appear since the angle between a protofilament and the longitude is small. However, lateral bonds between neighboring protofilaments lead to a twist-stretch coupling. This coupling will be disregarded here but treated in a later paper [14].

The total stretching energy per unit length of all the strands is $U_s = \Sigma_{i=1}^{11} U_{si}$, or

$$U_s = \frac{11u}{4}\left[(\epsilon^2 - \epsilon_p^2)^2 + (3\epsilon^2 - \epsilon_p^2)a^2\kappa^2 + \frac{3}{8}a^4\kappa^4\right], \tag{3}$$

where the curvature $\kappa = |\boldsymbol{\kappa}_\perp|$. Stretching resistance of the strands leads to bending resistance of the filament. The bending energy is isotropic, as expected for a cross section with symmetry higher than twofold.

The switch for twist in our model arises from a double-well potential per unit length (cf. [15]),

$$U_t = v\left[\frac{1}{4}a^4(\kappa_3^2 - \Omega_p^2)^2 - \bar{v}_1 a^4 \Omega_p^3 \kappa_3\right], \tag{4}$$

where we estimate $\Omega_p \approx 1$–$10\ \mu\mathrm{m}^{-1}$. Here we consider the simplest asymmetric double-well potential; $\bar{v}_1$ determines which well has lower energy.

Guided by the work of [11], we suppose there are cooperative interactions that give an energy penalty when neighboring subunits in the same protofilament are in different conformations (cf. the cooperative energy for *twist* of [15]). In the continuum limit, this penalty is $U_c = (w/2)\sum_{i=1}^{11}(\mathrm{d}\epsilon_i/\mathrm{d}S)^2 \approx (w/2)\sum_{i=1}^{11}(\mathrm{d}\epsilon_i/\mathrm{d}s)^2$, or,

$$U_c = \frac{11w}{2}\left[\epsilon'^2 + \frac{a^2}{2}(\kappa_1'^2 + \kappa_2'^2)\right], \tag{5}$$

where the prime denotes differentiation with respect to s. To interpret U_c, it is convenient to introduce the angle f from $\boldsymbol{\kappa}_\perp$ to $\hat{\mathbf{e}}_2$. Since $\kappa_1 = -\kappa\cos f$ and $\kappa_2 = \kappa\sin f$, we have $\kappa_1'^2 + \kappa_2'^2 = \kappa'^2 + \kappa^2(\tau - \kappa_3)^2$, where the torsion τ is related to twist by $\tau = \kappa_3 - f'$. Thus, the cooperative term U_c obtains its absolute minimum when ϵ and κ are uniform, and when the rod is either straight, $\kappa = 0$, or has torsion equal to the twist, $\tau = \kappa_3$. These conditions are necessary to achieve constant ϵ_i. Since the curvature κ and twist κ_3 do not uniquely determine the path of the centerline, the cooperative energy is crucial for defining the ground state of the filament.

The total energy is $E = \int ds[U_c + U_s + U_t + U_0]$, where we have approximated $dS \approx ds$. In this Letter we will consider the simplest case of an inextensible filament, $k_s \to \infty$, which implies $\epsilon = \epsilon_0$. The behavior of the model in this limit is qualitatively similar to that of the full model.

First we determine the ground states as a function of ϵ_0 and $\bar{v}_1$. We limit the discussion to helical and straight shapes, and neglect end effects.

With the condition $\kappa_3 = \tau$, the state of the filament is determined by minimizing the energy with respect to κ and κ_3, with $\epsilon = \epsilon_0$. Inspection of (3) reveals that the filament is straight when $|\epsilon_0| \geq \epsilon_p/\sqrt{3}$, and curved with $\kappa^2 a^2 = \kappa_0^2 a^2 \equiv 4(\epsilon_p^2/3 - \epsilon_0^2)$ when $|\epsilon_0| < \epsilon_p/\sqrt{3}$. To see why curved filaments arise, consider the stretching energy for a short segment of the filament (Fig. 1). If $\epsilon_0 = \epsilon_p$, then $\epsilon_i = \epsilon_p$ for all i minimizes the energy, and the filament is straight. If $\epsilon_0 = 0$, then the straight state with $\epsilon_i = 0$ is unstable, since the energy U_{si} of each of the 11 strands is at a local maximum [see Fig. 1(a) and 1(b)]. Stretching or compressing all 11 strands to make $\epsilon_i = \pm\epsilon_p$ will raise the energy of the inner core for finite k_s and is impossible for $k_s \to \infty$. The compromise that lowers the energy is to bend the element, maintaining the inner core at $\epsilon = 0$ [Fig. 1(b)]. Thus, curvature arises from an elastic incompatibility of the inner and outer core.

Minimizing the energy over twist leads to the condition

$$(\kappa_3/\Omega_p)^3 - \kappa_3/\Omega_p = \bar{v}_1. \tag{6}$$

Thus, the twist undergoes a discontinuous transition as $\bar{v}_1$ varies. Note that the curvature does not jump. If we had included the twist-stretch coupling mentioned above, both the curvature and twist would jump at a transition; a twist-stretch coupling also allows discontinuous transitions from helical to straight states [14].

Figure 2 shows the phase diagram for filament shape in terms of the parameters $\bar{v}_1$ and ϵ_0 governing the molecular switches. In the gray band it is energetically favorable for the filament to bend into a helix. The solid vertical line $\bar{v}_1 = 0$ marks the discontinuous transition from $\kappa_3 = -\Omega_p$ to $\kappa_3 = \Omega_p$. The twist potential has two minima, one stable and one metastable, in the region between the vertical dash-dot lines.

Figure 3 shows how the minimum-energy shape of a filament changes as $\bar{v}_1$ and ϵ_0 are varied along the path of the diagonal line in Fig. 2. The filament is first left-handed and straight, then undergoes a transition to a curved state (P_1). The curvature and twist change continuously through this transition. However, the curvature rises so steeply after P_1 that it could appear to jump. As we continue along the diagonal line of Fig. 2, we reach the discontinuous transition at $\bar{v}_1 = 0$ (P_2^-, P_2^+). At this point, the minimum-energy twist jumps to a right-handed value. (Metastable branches are also shown in Fig. 3.) As ϵ_0 continues to decrease along the diagonal line, the filament eventually undergoes a continuous transition to a straight state (P_3). In contrast with the theory of Calladine [2], our theory does not predict a universal relation between curvature and twist, nor does it predict a discrete set of states. A crucial test of our theory would be to observe the change in shape of a *single* filament as external conditions are varied.

To study the response of the filament to an external moment analytically, we take $\bar{v}_1 = 0$, and limit the discussion to helical solutions. Since the moment $\mathbf{M} = M\hat{\mathbf{z}}$ defines a natural space-fixed direction, we use Euler angles to parameterize the material frame. In the convention of Love [16], $\{\hat{\mathbf{e}}_\mu\}$ is generated from a space-fixed frame by first rotating by ψ about $\hat{\mathbf{z}}$, then rotating about the image of $\hat{\mathbf{y}}$ by θ, and then rotating by ϕ about the final image of $\hat{\mathbf{z}}$. Thus, a helix has parametrization

$$\mathbf{r}(s) = \left(\frac{\sin\theta}{\psi'}\sin(\psi' s), -\frac{\sin\theta}{\psi'}\cos(\psi' s), s\cos\theta\right), \tag{7}$$

with θ and ψ' constant. Note that helix handedness depends solely on the sign of ψ'. To find the shape, we use the principle of virtual work, $\delta E - \mathbf{M}\cdot[\delta\mathbf{Y}(L) - \delta\mathbf{Y}(0)] = 0$, where $\delta\Upsilon_\mu = -\epsilon_{\mu\nu\lambda}\hat{\mathbf{e}}_\nu \cdot \delta\hat{\mathbf{e}}_\lambda$ is the infinitesimal rotation of the frame $\{\hat{\mathbf{e}}_\mu\}$ at $s = L$ and $s = 0$. Taking the variations for arbitrary functions ψ, θ, and ϕ, and then specializing to the case of constant θ and ψ', we find $\phi' = 0$ and

$$\psi' \sin\theta(\psi'^2 \sin^2\theta - \kappa_0^2) = \frac{M}{\tilde{u}a^4}\sin\theta, \tag{8}$$

$$\psi' \cos\theta(\psi'^2 \cos^2\theta - \Omega_p^2) = \frac{M}{va^4}\cos\theta. \tag{9}$$

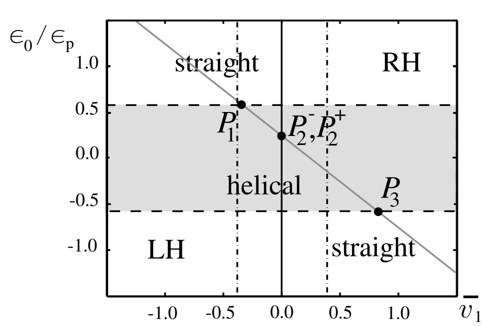

FIG. 2. Phase diagram for ground states. The vertical solid line separates left-handed and right-handed states. The vertical dash-dot lines define the limits of metastability for the twist potential. The diagonal line traces out the values of $\bar{v}_1$ and ϵ_0 used to calculate the curvature vs twist plot of Fig. 3.

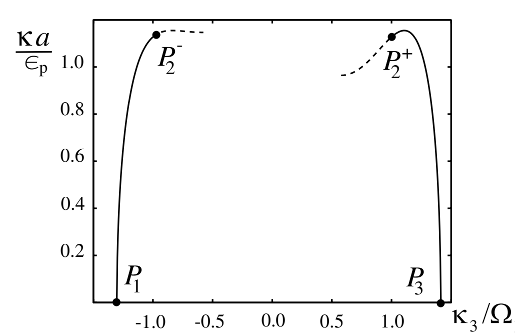

FIG. 3. Curvature vs twist, in dimensionless units. The solid line corresponds to minimum-energy states; the dashed lines correspond to metastable states. The parameters $\bar{v}_1$ and ϵ_0 vary along the diagonal line of Fig. 2.

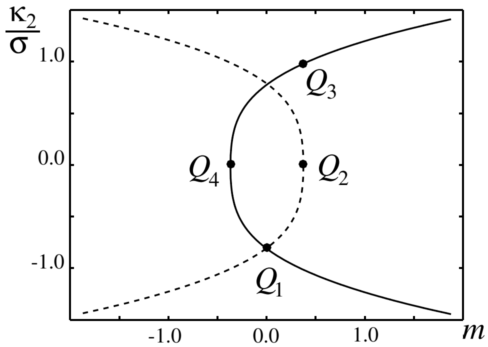

FIG. 4. Signed curvature κ_2 vs moment m, in dimensionless units, for $\tilde{u} = v$, $\theta_0 = 32°$. The solid line is the right-handed branch, and the dashed line is the left-handed branch (cf. Figure 5).

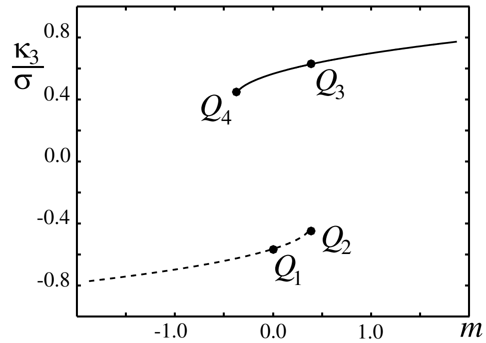

FIG. 5. Twist κ_3/σ vs moment m, in dimensionless units, for $\tilde{u} = v$ and $\theta_0 = 32°$.

We have defined $\tilde{u} = 33u/8$ and used the constancy of ϕ to choose $\phi = \pi/2$, which implies $\kappa_1 = 0$, $\kappa_2 = \psi' \sin\theta$, and $\kappa_3 = \psi' \cos\theta$. Eqs. (8) and (9) reduce to $\psi'^3/\sigma^3 - \psi'/\sigma = m$ and

$$\sin^2\theta = \frac{v}{\tilde{u} + v} + \left(\sin^2\theta_0 - \frac{v}{\tilde{u} + v}\right)\frac{\sigma^2}{\psi'^2} \qquad (10)$$

with $\sigma^2 = \kappa_0^2 + \Omega_{\mathrm{p}}^2$, $\tan\theta_0 = \kappa_0/\Omega_{\mathrm{p}}$, and $m = (\tilde{u} + v)M/(\tilde{u}v\sigma^3 a^4)$. Note that (8) and (9) do not determine the sign of θ; for every M, there are two physically different solutions related by $\kappa_2 \mapsto -\kappa_2$. For example, consider a filament in the plane $\theta = \pi/2$ with a bistable potential for curvature but no twist. For zero external moment the filament will be an arc of a circle with either sign of κ_2; suppose $\kappa_2 > 0$. Applying a moment to decrease the curvature will cause the filament to first deform smoothly, and then snap into a shape with $\kappa_2 < 0$.

There is a rich array of possibilities for polymorphic transitions under an external moment [14]. We consider in detail only the case of $\tilde{u} = v$ with $\theta_0 = 32°$, the approximate pitch angle of the normal state. Zero external moment corresponds to the point Q_1 in Figs. 4 and 5. As the moment increases, the shape changes smoothly through metastable states until Q_2, where *both* κ_2 and κ_3 jump to the values at Q_3. In this case, $\kappa_2 = 0$ at Q_2; when $\theta_0 > 45°$, κ_2 is nonzero at the transition. As the moment increases further, the shape continues to change smoothly. If the moment then decreases, the shape deforms smoothly until Q_4, where there is another transition in κ_2 and κ_3.

To conclude, we have introduced a new continuum model for flagellar filaments that accounts for the alternate stable conformations of the protein subunits. The predictions of the model differ from those of previous models [2,15], and may be readily tested by new single-molecule experiments on the response of a single filament to changes in solvent condition and end loading.

We thank H. Berg, C. Calladine, D. DeRosier, A. Goriely, K. Namba, A. Needleman, L. Turner and C. Wolgemuth for helpful conversations. We are especially grateful to G. Huber for many important discussions. This work is supported in part by National Science Foundation Grant Nos. CMS-0093658 and NIRT-0404031, and the Brown University MRSEC. T. R. P. thanks the Aspen Center for Physics for hospitality while some of this work was completed.

[1] S. Asakura, Advan. Biophys. (Japan) **1**, 99 (1970).
[2] C. R. Calladine, Nature (London) **255**, 121 (1975).
[3] L. Turner, W. S. Ryu, and H. C. Berg, J. Bacteriol. **182**, 2793 (2000).
[4] R. M. Macnab and M. K. Ornston, J. Mol. Biol. **112**, 1 (1977).
[5] H. Hotani, J. Mol. Biol. **156**, 791 (1982).
[6] R. Kamiya and S. Asakura, J. Mol. Biol. **106**, 167 (1976).
[7] H. C. Hyman and S. Trachtenberg, J. Mol. Biol. **220**, 79 (1991).
[8] Y. Mimori, I. Yamashita, K. Murata, Y. Fujiyoshi, K. Yonekura, C. Toyoshima, and K. Namba, J. Mol. Biol. **249**, 69 (1995).
[9] S. Kanto, H. Okino, S. I. Aizawa, and S. Yamaguchi, J. Mol. Biol. **219**, 471 (1991).
[10] Y. Mimori-Kiyosue, F. Vonderviszt, I. Yamashita, Y. Fujiyoshi, and K. Namba, Proc. Natl. Acad. Sci. U.S.A. **93**, 15 108 (1996).
[11] F. A. Samatey, K. Imada, S. Nagashima, F. Vonderviszt, T. Kumasaka, M. Yamamoto, and K. Namba, Nature (London) **410**, 331 (2001).
[12] K. Yonekura, S. Maki-Yonekura, and K. Namba, Nature (London) **424**, 643 (2003).
[13] I. Yamashita, K. Hasegawa, H. Suzuki, F. Vonderviszt, Y. Mimori-Kiyosue, and K. Namba, Nat. Struct. Biol. **5**, 125 (1998).
[14] S. V. Srigiriraju and T. R. Powers (to be published).
[15] R. E. Goldstein, A. Goriely, G. Huber, and C. W. Wolgemuth, Phys. Rev. Lett. **84**, 1631 (2000).
[16] A. E. H. Love, *A Treatise on the Mathematical Theory of Elasticity* (Dover, New York, 1944), 4th ed.